Synthesis and Phase Transitions of Thermotropic Liquid Crystalline Copolyesters with Phosphorus–Containing Pendent Bulky Groups

DIANA SERBEZEANU[*], **TACHITA VLAD-BUBULAC, CORNELIU HAMCIUC, MAGDA AFLORI, MARIA BRUMA**
"Petru Poni" Institute of Macromolecular Chemistry, 14A Aleea Grigore Ghica Voda, 700487, Iasi, Romania

A series of thermotropic liquid crystalline phosphorus-containing copolyesters was prepared by polycondensation reaction starting from various ratios of 2-(6-oxido-6H-dibenz<c,e><1,2>oxaphosphorin-6-yl)-1,4-benzene diol, ***1****, terephthaloyl bis-(4-oxybenzoyl-chloride),* ***2****, and, 1,12-dodecanediol,* ***3****. The molar ratio of aromatic bisphenol to aliphatic diol was varied in order to generate copolyesters with tailored physico-chemical properties. The chemical structure of the synthesized polymers has been confirmed by Fourier transform infrared and* ^{1}*H NMR spectroscopy. The phase transitions of the phosphorus-containing copolyesters have been investigated by differential scanning calorimetry, polarizing optical microscopy and X-ray diffraction measurements, structure–properties relationships being established and discussed.*

Keywords: phosphaphenanthrene; phase transitions; structure-property relations

Thermotropic liquid-crystalline polymers (TLCPs) have generated much interest in material science in recent years because of their various industrial and commercial applications, such us optical devices and engineering plastics [1]. The main chain wholly aromatic thermotropic polyesters have received considerable interest for technological applications because of their good thermal stability, excellent chemical resistance, high glass transition temperatures, in addition to good processing and mechanical properties [2]. In order to design aromatic polyesters with lowered melting transitions, which allows appearance of the liquid crystalline phases below the temperatures corresponding to the thermal degradation or isotropization, several approaches have been taken into consideration, namely, copolymerization, insertion of flexible spacer, use of laterally attached bulky groups, introduction of bent or crankshaft sequences etc. [3,4]. The most typical spacer segments employed are polymethylene units $(CH_2)_n$ of varying length *n*. It has been demonstrated that a higher value of *n* decreased the phase transitions of such copolymers with a minimum sacrifice of the thermal stability [5]. Introduction of lateral bulky groups to *p*-oriented monomers has also been applied to lower the melting points of TLCPs. The incorporation of phosphaphenanthrene bulky structure (9,10-dihydro-9-oxa-10-phosphaphenanthrene-10-oxide (**DOPO**)) into polymers resulted in polymers with good solubility, resonable thermal stability, good adhesion, low birefringence etc. [6–8]. **DOPO**–containing polymers have received significant attention in the recent years because they are considered to be effective flame retardants, as demonstrated in recent studies [9–12]. Phosphorus-containing polymers tend to char rather than burn, thus, the char yield provides a diffusion barrier of gaseous products to the flame, shields the polymer surface from heat and oxygen, and reduces the production of combustible gas during polymer degradation [13]. In addition, phosphorus-containing polymers meet the requirements of low toxicity and low smoke during burning for environmental and health considerations [14,15].

Previously, we had successfully applied the concept of achieving and controlling the thermal decomposition, flame retardancy, phase transitions and crystallinity degree of aromatic-aliphatic copolyesters by combination of phosphorus-containing monomer and aliphatic moieties into aromatic mesogenic core [5,16,17]. It has been found that the copolymers having shorter flexible spacer groups tend to form a nematic mesophase, while the copolymers having longer flexible spacer groups tend to form a smectic mesophase.

In the present work we describe the results of the polycondensation of an aromatic bisphenol containing phosphaphenanthrene groups, namely 2-(6-oxido-6H-dibenz<c,e><1,2>oxaphosphorin-6-yl)-1,4-benzene diol, **1**, with a diacid chloride containing two preformed ester groups, **2**, and 1,12-dodecanediol, **3**. The properties of the polymers, such as solubility, thermal stability and phase transitions have been investigated.

Experimental part

Materials and methods

DOPO was purchased from Chemos GmbH, Germany. Benzoquinone, 4-hydroxybenzoic acid, terephthalic acid, and compound **3** were purchased from Aldrich and used as received. Compounds **1** and **2** have been synthesized according to methods previously reported in the literature [16,18]. All other reagents were used as received from commercial sources or they were purified using standard methods.

Measurements

Melting points of the monomers and intermediates were measured on a Melt-Temp II (Laboratory Devices). FT-IR spectra were recorded on a Bruker Vertex 70 at wave numbers ranging from 400 to 4000 cm^{-1}. Samples were mixed with KBr and pressed into pellet form. ^{1}H NMR (400 MHz) spectra were performed at room temperature on a Bruker Avance DRX 400 spectrometer. The polymer was dissolved in mixed solvents of $CDCl_3$ and CF_3COOD ($CDCl_3$:CF_3COOD = 9:1, v/v). The differential scanning calorimetry (DSC) analysis was carried out using a Perkin-Elmer Pyris Diamond instrument using nitrogen as a carrier gas at a flow rate of ca 10 mL/min. All samples were first heated from room temperature to 350°C using a heating rate of 10 °C/min, then cooled to 20°C at a cooling rate of

---

[*] *email: diana.serbezeanu@icmpp.ro; Tel.: +40-232-217454*

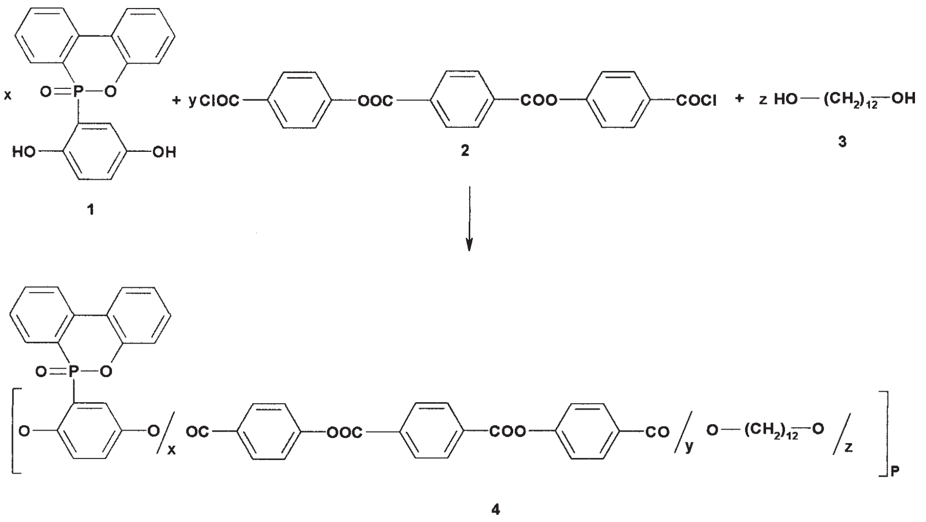

Scheme 1
Synthesis of the copolyesters **4**

	x	y	z
4a	1	1	0
4b	0.75	1	0.25
4c	0.5	1	0.5
4d	0.25	1	0.75
4e	0	1	1

10 °C/min. The melting temperatures and the liquid crystalline phase transition temperatures of copolyesters **4** were taken as maximum of endothermic peaks. Polarized light microscopy (PLM) was carried out with an Olympus BH-2 polarized light microscope fitted with a THMS 600/HSF9I hot stage, at a magnification of 200× or 400×. The wide-angle X-ray diffraction (WAXD) experiments at room temperature and variable temperature XRD were performed on a D8 Advance Bruker AXS diffractometer using a CuKα source with an emission current of 36 mA and a voltage of 30 kV. Scans were collected over the $2\theta = 2$–40 range using a step size of 0.01° and a count time of 0.5 s/step. The heating and cooling rates in all WAXD experiments were 0.5°C/s.

Synthesis of the polymers

The synthetic route of the polymers **4** is depicted in scheme 1. The experimental details are described below using polymer **4a** as an example. In a 100 mL flask equipped with magnetic stirrer and nitrogen-inlet and outlet 0.324 g (0.001 mol) of aromatic bisphenol **1**, 0.443 g (0.001 mol) of diacid chloride **2** and 5 mL *o*-dichlorobenzene, were introduced. The reaction mixture was refluxed for 20 h, it was cooled to room temperature, washed with methanol, filtered off and dried at 100°C for 5 h. The polymer was purified by reprecipitation in methanol from chloroform/trifluoroacetic acid (9/1, vol./vol.) and dried at 80 °C for 8 h under vacuum. Yield: 91%. The same procedure was used to synthesize the homopolyester **4e** by taking into reaction the aliphatic diol **3** (0.202 g, 0.001 mol) instead of **1**. Copolyesters **4b**, **4c**, and **4d** were synthesized according to the amount of 0.243 g (0.00075 mol), 0.162 g (0.0005 mol) or 0.081 g (0.00025 mol) of **1** and 0.0505 g (0.00025 mol), 0.101 g (0.0005 mol) or 0.151 g (0.00075 mol) of **3**, based on the above procedure, using 0.443 g (0.001 mol) compound **2** for each polymer.

Results and discussions

Synthesis of the polymers and general characterization

The structure of the resulting polymers has been investigated by FT-IR and ^{1}H NMR spectroscopy. For example, the FT-IR spectrum of polymer **4d** is shown in figure 1. The most important absorption bands are associated with aromatic C–H (3065 cm $^{-1}$, stretching vibration), aliphatic C–H (2917 cm $^{-1}$ and 2850 cm $^{-1}$, asymmetric and symmetric stretching vibrations), C=O (1733 cm $^{-1}$, stretching vibration), ester C–O–C (1259 cm^{-1} and 1015 cm $^{-1}$, asymmetric and symmetric stretching vibrations), P–O–Ar (930 cm $^{-1}$ and 1162 cm $^{-1}$, stretching vibrations), P–Ar (1472 cm^{-1}), P=O (1199 cm^{-1}), aromatic C–H (758 cm $^{-1}$, deformation vibration caused by the 1,2-disubsituted aromatic DOPO rings), aromatic C–H (717 cm $^{-1}$, deformation vibration from aromatic terephthaloyl ring) [16,19,20]. Aromatic C=C bands were found at 1604 cm $^{-1}$ and 1502 cm $^{-1}$.

The ^{1}H NMR spectrum of the polymer **4d** exhibited characteristic peaks in the region of 8.38-6.87 ppm due to the presence of the aromatic protons. The peaks that characterize the methylene groups of the unit structure appeared at 4.38 ppm (O-CH_2, 4H), 1.8 ppm (O-CH_2-CH_2, 4H) and the peak characterizing the other methylene groups of the structural unit (CH_2, 16H) appeared in the region of $\delta \cong 1.47$–1.31 ppm.

Polymers **4** were only partially soluble in organic solvents like N,N-dimethylformamide, N-methylpyrrolidone or dimethylsulfoxide due to the rigidity of the segment coming from the diacid chloride **2** which contains three *p*-phenylene rings connected by ester units. The macromolecular chains can adopt a linear conformation and allowed a strong packing that reduced the solubility. The solubility becomes

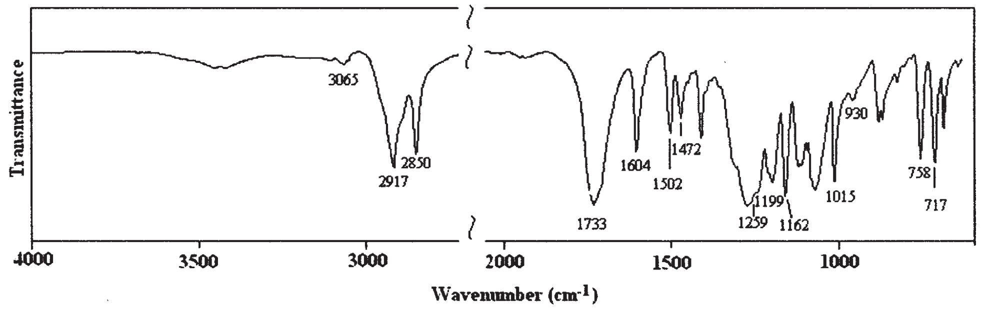

Fig. 1. FT-IR spectrum of polymer **4d**

Table 1
PHASE TRANSITION TEMPERATURES OF SYNTHESIZED POLYMERS **4**

Polymer	Transition temperatures from DSC[a)] (°C)	Transition temperatures from PLM[b)] (°C)
4a	K261LC*(–)I	K385LC(–)I
4b	$K_1$164$K_2$181LC*(–)I	K237LC330I
4c	$K_1$162$K_2$188LC*(–)I	K246LC310I
4d	$K_1$179 $K_2$198(206)LC*(–)I	K232LC295I
4e	$K_1$158 $K_2$169(188)LC*(–)I	K191LC238I

a) Peak temperatures from DSC taken as the phase transition temperature; [b)] Phase transition temperature taken from polarized light microscopy observation, first heating cycle at a heating rate of 10°C/min; K, K_1, K_2-solids, I–isotropic phase, LC, LC*–liquid crystalline phases; (–) Peak temperature not observed by DSC.

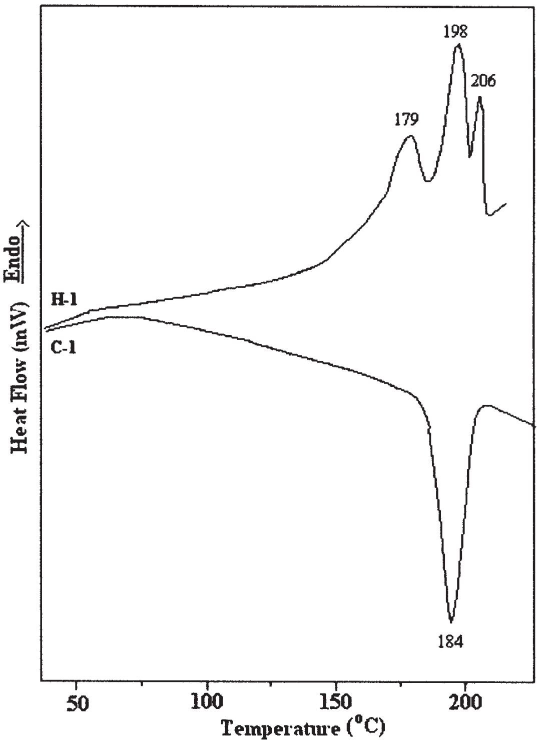

Fig. 2. DSC thermogram of polymer **4d**, H-1, first heating, C-1, first cooling.

better by increasing the content of phosphorus-containing bisphenol which possesses a polar P=O group and a bulky structure [21–23].

Phase transition investigations

The thermal properties and the phase transition temperatures of the polymers **4**, obtained during the first heating-cooling cycle, have been determined by DSC, and the data for these transitions are summarized in table 1. The data listed in table 1 revealed a considerable effect of molecular structure on the melting temperatures and mesomorphic properties as will be discussed in this section. Figure 2 shows the first heating-cooling DSC curves of the polymer **4d** at a heating/cooling rate of 10°C/min. The DSC curves showed multiple melting endotherms, a phenomenon previously reported as a feature in common for liquid crystalline polyesters [24–27], which was attributed to the presence of different crystal structures [28] or to crystal reorganization [29] or to different components of the morphology formed in multiple stages of crystallization [30]. The as-synthesized copolymer **4d** (fig. 2, H-1 curve) exhibited multiple melting endotherms (T ≈ 179, 198, 206°C). Upon cooling, the copolymer **4d** showed a sharp crystallization exotherm (T ≈ 184 °C) that corresponds to the crystallization temperature. The DSC trace of the polymer **4a** did not show a multiple melting behavior, but a melting endotherm appeared at about 261 °C. As seen from table 1, for the first DSC heating scan of the copolymers **4b–4e**, the melting starts close to 160 °C. Therefore, we may assume that the endotherm corresponds to the melting process of the terephthaloyl-bis(4-oxyphenylene carbonyl)-dodecandiol segments [17].

Polarizing light microscopy (PLM) was used to identify the liquid crystalline phases and to complement the phase transitions observed by DSC. Optical micrographs of different textures are shown in figure 3. The data of the mesomorphic transition temperatures (K→LC→I) are given in table 1. A suitable amount of sample for each polymer was charged between two clean glass plates. The samples were heated to clearing point, which is considered as the liquid crystalline-to-isotropic state transition. The transition temperatures from crystal to liquid crystalline melt were in the range 191–385 °C and depend slightly on the aliphatic content, polymer **4a** having the highest value for the transition K→LC (385 °C). In the case of the polymer **4a** the LC→I transition temperature was not detected by PLM investigation because this polymer had too high T_i to match the limiting temperature of the hot stage of PLM (400 °C). The LC→I transition temperature for polymers **4b–4e** was in the range 238–330 °C and greatly depends on the content of aliphatic diol. The transition temperatures of the polymers **4** obtained by PLM were compared with those measured by DSC measurements. These two methods gave comparable results as seen in table 1. The observed differences could be explained by the variation of heating-cooling rate, amounts of the sample used for the measurements, or the presence of the different atmosphere (nitrogen, in the case of DSC, and air, in the case of the PLM investigation). Upon heating all as-synthesized polymers **4** formed fine textures (fig. 3a), difficult to ascribe to a smectic or nematic phase,

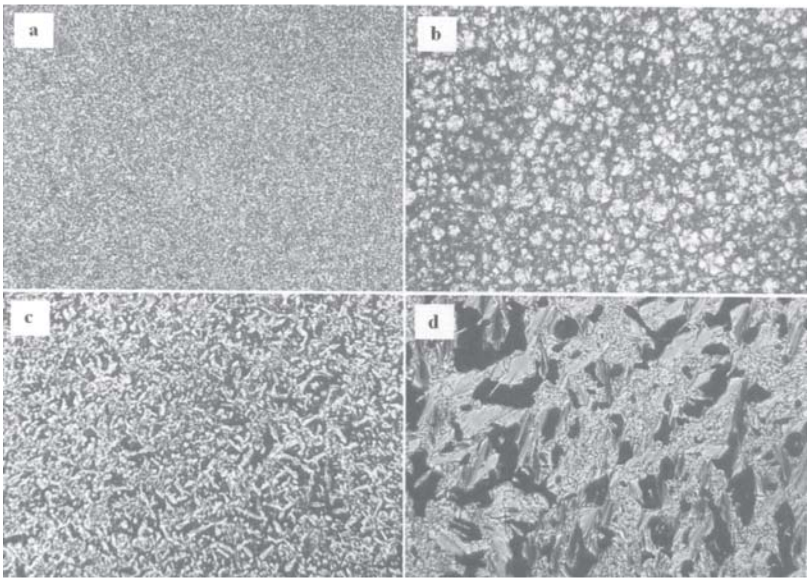

Fig. 3. Optical micrographs of polymers **4**: polymer **4c** heating cycle at 299 °C, fine texture (a); polymer **4e**, heating cycle at 219 °C, showing fingerprint droplets (b); polymer **4d**, cooling cycle at 280 °C, (batonnets growing from the isotropic phase (c); polymer **4d**, cooling cycle at 227 °C, (fan-shaped texture) (d).

but similar to those reported for thermotropic polymers based on terephthaloyl-bis(4-oxyphenylene carbonyl) units [24–26]. After annealing of the sample **4e** at 219°C for 10 min a kind of interesting fingerprint droplets appeared from the fine granular texture (fig. 3b). Upon cooling from the isotropic state, the polymers **4** behave different as a function of the aliphatic content. The flexible methylene spacer groups separate the mesogenic alignment, thereby reducing the overall rigidity. Thus, the polymers **4d** and **4e** containing a higher ratio of 1,12-dodecanediol seem to form textures typical of smectic phases, whereas the polymers with smaller content of methylene groups in the structural unit (**4b** and **4c**) loose the ability to organize into more ordered phases and displayed only fine threaded textures, typical of nematic phases. Upon cooling the copolymer **4d** from the isotropic state (300 °C) at a rate of 5°C/min, some very tiny birefringent batonnets start to appear in the vicinity of 290°C. On continuing cooling to 280°C these small batonnets grow and populate the whole microscopic view (fig. 3c). When the temperature approaches the value of 250°C the nematic disclinations structures transform into more ordered phases showing few fan-shaped textures which are suggestive of a smectic A phase (fig. 3d).

The mesophase of the polymers was also characterized through X-ray diffraction measurements. The XRD data (percentage crystallinity, peaks intensity, d-spacing values, and Bragg angles) of the polymers **4** obtained at room temperature are summarized in table 2. Figure 4 shows a set of one-dimensional WAXD patterns detected at room temperature for this series of phosphorus-containing polyesters **4** with different contents of aliphatic units in the main chain. At room temperature the polymers **4a** and **4b** showed diffraction peaks only in the wide-angle region. Thus, in the case of polymer **4b** the scattering halos at around 2θ=15, 19.3, 19.7 and 23.8° revealed a typical semicrystalline behavior [27]. The two broad diffused reflections centered at around 19.68 ° and 23.58 ° in polymers **4a–4c** transformed into stronger and sharper reflections in polymers **4d** and **4e** (fig. 4), which permitted us to conclude that an intermolecular distance of the polymers became smaller by decreasing the content of bulky phosphorus-containing groups laterally attached to the macromolecular chains. At room temperature the polymers **4d** and **4e** possess strong and sharp low-angle diffraction peaks at 2θ=2.8° (*d*-spacing = 33.6 Å) and 2.5 ° (*d*-spacing = 35.8Å), respectively, suggesting a layer ordered crystalline structure. Furthermore, the peaks at low-angle were still visualized after heating the sample to mesomorphic state (200 °C) supporting the PLM observations that at this temperature the polymers **4d** and **4e** displayed textures characteristic for smectic phases (figs.3, 5, table 1). The percent crystallinity of the polymers was determined by bisecting the experimental plot into the crystalline domain and amorphous domain by curve fitting. The areas under the crystalline and amorphous domain are determined computationally and the percentage crystallinity was calculated. The percentage crystallinity varies from 24 to 40% depending upon aliphatic segment content in the polymer. The percentage crystallinity decreased upon increasing the content of aromatic bisphenol from 40%, in the case of polyester **4e** to 24% in the case of the copolyester **4b** which contained the smallest quantity of aliphatic diol in the structural unit of the macromolecular chain.

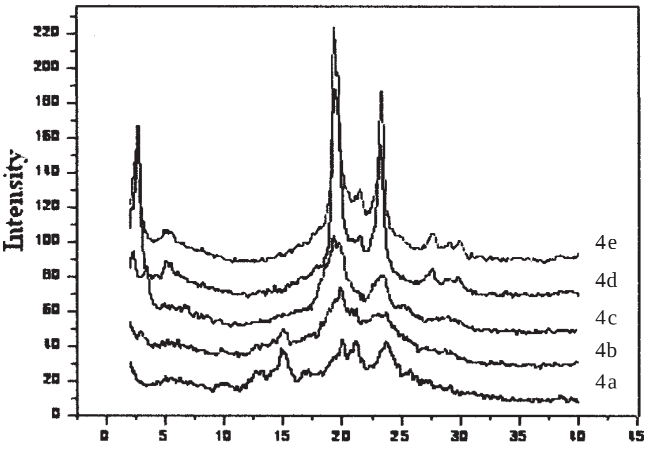

Fig. 4. Wide-angle X-ray diffractogram of polymers **4**, samples at room temperature

To verify the nature of the phases for the copolymer **4d**, temperature-resolved WAXD patterns were generated and analyzed. The heating and cooling results of WAXD diffractograms confirmed the transitions listed in table 1. The cell parameter refinement has been performed by using EVA software from the Diffract Plus package and the ICDD PDF-2/Release 2005 database, by tailoring the parameters for profile fitting: background degree, asymmetry, broadening, and Lorentz width.

Figure 5 shows a series of the X-ray diffractometer scans of the polymer **4d** sample, recorded as a function of temperature from room temperature to the mesomorphic

Table 2
OBSERVED X-RAY DIFFRACTION DATA FOR POLYESTERS **4**

Polymer	Peak (2θ) (°)	d-Spacing (Å)	Intensity (%)	Crystallinity (%)
4a	15	5.9	91	26
	19.3	4.6	79	
	19.7	4.5	100	
	23.8	3.7	89	
4b	14.8	6.0	64	24
	19.9	4.4	90	
	23.0	3.9	75	
4c	3.4	26.3	62	27
	19	4.6	100	
	23.4	3.8	60	
4d	2.8	33.6	79	38
	19.4	4.6	74	
	23.3	3.8	100	
4e	2.5	35.8	58	40
	19.4	4.6	100	
	23.4	3.8	69	

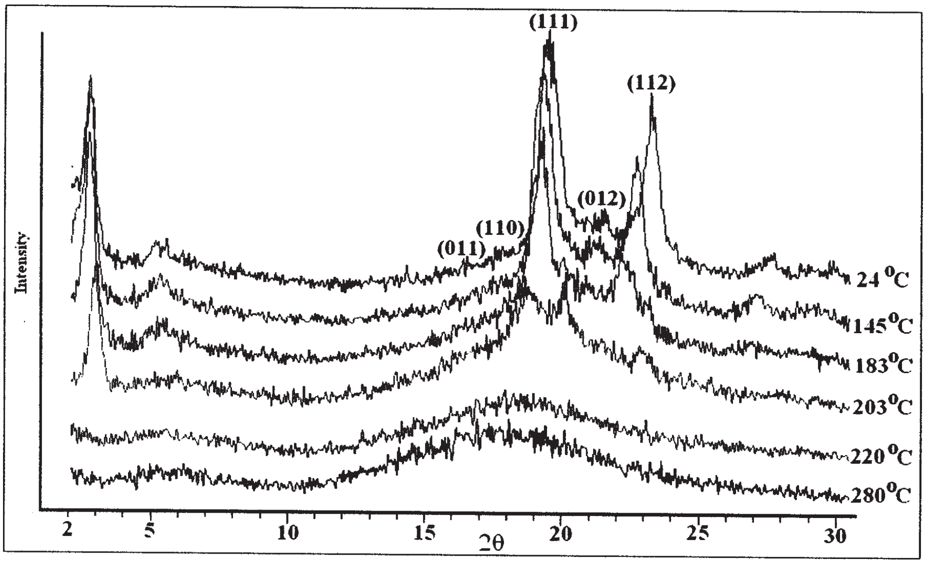

Fig. 5. XRD pattern of the polymer **4d** at different temperatures

state. The polymer **4d** exhibits a relatively sharp diffraction pattern for a polymer, but is comparable with those obtained for similar polymers based on terephthaloyl-bis(4-oxyphenylenecarbonyl)units [28]. The cell parameters were refined at 24°C and we found an orthorhombic structure that was indexed with unit cell parameters of *a* = 8.47 Å, *b* =6.06 Å, and *c* =11.98Å. Changes in the X-ray diffraction patterns in figure 5 can be seen near 145 and 183°C, which are consistent with the DSC results from table 1, where two endothermic peaks are listed for the same sample at 198 and 206°C, respectively. On heating, at the first melting point, the orthorhombic structure persists at 145°C, with the 111 and 112 peaks moving to lower 2θ values. At the second melting point, around 183°C, *a* dimension of the orthorhombic structure expands, while *b* and *c* dimensions remain almost constant (the chain axis is in the c direction). At this temperature the volume of the unit cell increases by approximately 6 %, which originates mostly from the increase in the cross-sectional area per chain. The diffraction peaks disappear above 220 °C and a single major diffraction halo dominates the scan, which suggests that the macromolecules in these phases have conformational mobility and a relatively high degree of disorder. By lowering the temperature, polymer **4d**, recovers the orthorhombic phase, verifying that the high-temperature phase is not a decomposition product, but a mobile phase.

Conclusions

The present work reports the synthesis of a series of main chain thermotropic liquid crystalline polyesters with phosphorus-containing pendent bulky groups. The chemical structure of the products was confirmed by FT-IR and H NMR spectroscopy. The phase transitions of the polymers **4** were investigated by DSC, PLM and X-ray diffraction measurements. It has been revealed that the phase transitions temperatures decreased by increasing the content of aliphatic diol. Textures typical for smectic phases were identified for the polymers **4d** and **4e** with a higher content of methylene moieties. The presence of the phases with high conformational mobility at higher temperatures was confirmed by the existence of only broad, diffuse X-ray reflections.

Acknowledgements: This work was supported by CNCSIS-UEFISCSU, project number PN II-RU 657/2010. The authors would like to thank Dr. Daniel Timpu for X-ray analysis of the copolyesters.

References

1.DONALD, A.M., WINDLE, A.H., HANNA, S., In Liquid crystalline polymers,; 2nd Ed. Cambridge University Press: Cambridge, p. 504–543, 2006

2.GREINER, A., SCHMIDT, H.-W., Aromatic main chain liquid crystalline polymers, In Handbook of liquid crystals volume 3, High molecular weight liquid crystals, Demus, D., Goodby, J.W., Gray, G.W., Spiess, H.W. and Vill, V., eds., Wiley-VCH: New York, p. 3–23, 1998

3.DOMSZY, R.C., SHANNON, P.J., Macromolecules, **23**, 1990, p. 2790.

4.XU, Y., YANG, Q., SHEN, Z., CHEN, X., FAN, X., ZHOU, Q., Macromolecules, **42**, 2009, p.2542

5.SERBEZEANU, D., VLAD-BUBULAC, T., HAMCIUC, C., AFLORI, M., J. Polym. Sci. Part A Polym. Chem., **48**, 2010, p. 5391

6.VLAD-BUBULAC, T., HAMCIUC, C., PETREUS, O., LISA, G., Mater. Plast. (Bucharest), **44**, 2007, p. 284

7.HAMCIUC, C., VLAD-BUBULAC, T., PETREUS, O., LISA, G., Eur. Polym. J., **43**, 2007, p. 980

8.VLAD-BUBULAC, T., HAMCIUC, C., Polym. Eng. Sci., **50**, 2010, p. 1028

9.WANG, X., HU, Y., SONG, L., XING, W., LU, H., LV, P., JIE, G., Polymer, **51**, 2010, p. 2435

10.DU, X.-H., WANG, Y.-Z., CHEN, X.-T., TANG, X.-D., Polym. Degrad. Stab., **88**, 2005, p. 52

11.LIU, Y.L., WU, C.S., HSU, K.Y., CHANG, T.C., J. Polym. Sci. Part A Polym. Chem., **40**, 2002, p. 2329

12.CANADELL, J., MANTECON, A., CADIZ, V., J. Polym. Sci. Part A Polym. Chem., **45**, 2007, p. 1980

13.LU, S. Y., HAMERTON, I., Prog. Polym. Sci., **27**, 2002, p. 1661

14.LIANG, H., SHI, W., Polym. Degrad. Stab., **84**, 2004, p. 525

15.PETREUS, O., POPESCU, F., BARBOIU, V., ROSESCU, L., J. Macromol. Sci. Chem., **A25**, 1988, p. 1033

16.VLAD-BUBULAC, T., HAMCIUC, C., Polymer, **50**, 2009, p. 2220.

17.SERBEZEANU, D., VLAD-BUBULAC, T., HAMCIUC, C., AFLORI, M., Macromol. Chem. Phys., **211**, 2010, p. 1460.

18.WANG, C.S., LIN, C., Polymer, **40**, 1999, p. 4387

19.SOCRATES, G. In Infrared and Raman Characteristics Groups Frequencies: Tables and Charts, 3rd Ed. John Wiley & Sons: Chichester,p. 157 2004

20.THOMAS, L.C. In Interpretation of the Infrared Spectra of Organophosphorus Compounds, Heyden, London, 1974

21.CHANG, S. J., CHANG, F. C., J. Appl. Polym. Sci., **72**, 1999, p. 109.

22.SUN, Y. M., HUNG, A.Y.C., WANG, C. T., J. Appl. Polym. Sci., **85**, 2002, p. 2367

23.LEVCHIK, S.V., WEIL, E.D., Polym. Int., **54**, 2005, p. 11

24.IGNATIOUS, F., LENZ, R.W., KANTOR, S.W., Macromolecules, **27**, 1994, p. 5248

25.MCCARTHY, T.F., LENZ, R.W., KANTOR, S.W., Macromolecules, **30**, 1997, p. 2825

26.SKOVBY, M.H.B., LESSEL, R., KOPS, J., J. Polym. Sci. Part A Polym. Chem., **28**, 1990, p. 1980

27.MARIN, L., COZAN, V., BRUMA, M., GRIGORAS, V.C., Eur. Polym. J., **42**, 2006, p. 1173

28.LIN, L.L., HONG, J.L., Polymer, **41**, 2000, p. 4501

Manuscript received: 17.03.2011